

Non-Markovian dynamical solver for efficient combinatorial optimization

Haijie Xu(徐海杰) and Zhe Yuan(袁喆)

Citation: Chin. Phys. B, 2026, 35 (**2**): 027503. DOI: 10.1088/1674-1056/ae1fea
http://cpb.iphy.ac.cn; http://iopscience.iop.org/cpb

What follows is a list of articles you may be interested in

Chemical pressure manipulation of ferromagnetism in magnetic semiconductor $Ba(Zn,Mn,Cu)_2As_2$

Xueqin Zhao(赵雪芹), Jinou Dong(董金瓯), Lingfeng Xie(谢玲凤), Xun Pan(潘洵), Haoyuan Tang(唐浩原), Zhicheng Xu(徐之程), and Fanlong Ning(宁凡龙)
Chin. Phys. B, 2025, 34 (**10**): 107510. DOI: 10.1088/1674-1056/addbce

Magnetic and magnetocaloric effect of $Er_{20}Ho_{20}Dy_{20}Cu_{20}Ni_{20}$ high-entropy metallic glass

Shi-Lin Yu(于世霖), Lu Tian(田路), Jun-Feng Wang(王俊峰), Xin-Guo Zhao(赵新国), Da Li(李达), Zhao-Jun Mo(莫兆军), and Bing Li(李昺)
Chin. Phys. B, 2024, 33 (**5**): 057502. DOI: 10.1088/1674-1056/ad1a94

Crystal growth of $CeMn_{0.85}Sb_2$: Absence of magnetic order of Ce-sublattice

Yong Li(李勇), Shan-Shan Miao(苗杉杉), Hai Feng(冯海),Huai-Xin Yang(杨槐馨), and You-Guo Shi(石友国)
Chin. Phys. B, 2023, 32 (**6**): 067501. DOI: 10.1088/1674-1056/acc060

Effects of phosphorus doping on the physical properties of axion insulator candidate $EuIn_2As_2$

Feihao Pan(潘斐豪), Congkuan Tian(田丛宽), Jiale Huang(黄嘉乐), Daye Xu(徐大业), Jinchen Wang (汪晋辰), Peng Cheng(程鹏), Juanjuan Liu(刘娟娟), and Hongxia Zhang(张红霞)
Chin. Phys. B, 2022, 31 (**5**): 057502. DOI: 10.1088/1674-1056/ac5d2c

Magnetic properties and magnetocaloric effects in $(Ho_{1-x}Y_x)_5Pd_2$ compounds

X F Wu(武小飞), C P Guo(郭翠萍), G Cheng(成钢), C R Li(李长荣), J Wang(王江), Y S Du(杜玉松), G H Rao(饶光辉), Z M Du(杜振民)
Chin. Phys. B, 2019, 28 (**5**): 057502. DOI: 10.1088/1674-1056/28/5/057502

Non-Markovian dynamical solver for efficient combinatorial optimization

Haijie Xu(徐海杰)[1,2] and Zhe Yuan(袁喆)[2,3,†]

[1] *Center for Advanced Quantum Studies and School of Physics and Astronomy, Beijing Normal University, Beijing* 100875, *China*
[2] *Interdisciplinary Center for Theoretical Physics and Information Sciences, Fudan University, Shanghai* 200433, *China*
[3] *State Key Laboratory of Surface Physics, Fudan University, Shanghai* 200433, *China*

(Received 7 November 2025; revised manuscript received 15 November 2025; accepted manuscript online 17 November 2025)

We incorporate a non-Markovian feedback mechanism into the simulated bifurcation method for dynamical solvers addressing combinatorial optimization problems. By reinjecting a portion of dissipated kinetic energy into each spin in a history-dependent and trajectory-informed manner, the method effectively suppresses early freezing induced by inelastic boundaries and enhances the system's ability to explore complex energy landscapes. Numerical results on the maximum cut (MAX-CUT) instances of fully connected Sherrington–Kirkpatrick (SK) spin glass models, including the 2000-spin K_{2000} benchmark, demonstrate that the non-Markovian algorithm significantly improves both solution quality and convergence speed. Tests on randomly generated SK instances with 100 to 1000 spins further indicate favorable scalability and substantial gains in computational efficiency. Moreover, the proposed scheme is well suited for massively parallel hardware implementations, such as field-programmable gate arrays, providing a practical and scalable approach for solving large-scale combinatorial optimization problems.

Keywords: non-Markovian dynamics, simulated bifurcation, combinatorial optimization, maximum cut (MAX-CUT) problem, spin glass

PACS: 75.10.Nr, 02.60.Pn, 05.10.–a

DOI: 10.1088/1674-1056/ae1fea **CSTR:** 32038.14.CPB.ae1fea

1. Introduction

Combinatorial optimization problems (COPs) play a central role in numerous fields of science and engineering, yet remain notoriously challenging for conventional computing architectures. Such problems require identifying the optimal configuration from an exponentially large solution space, which is generally formulated through a cost or objective function. A considerable portion of these problems fall into the class of non-deterministic polynomial-time (NP)-complete problems, which are among the most computationally intractable in NP.[1] The significance of this classification lies in the fact that any NP problem can be polynomially reduced to an NP-complete problem, implying that improvements in solving even a single NP-complete problem could have broad impact. As a representative example, the maximum cut (MAX-CUT) problem is closely connected to a wide range of applications including circuit layout design,[1–3] machine learning,[4] and image segmentation.[5] Thus, it is an important problem in its own right.

A common approach to addressing COPs is to map the solution onto the ground state of a physical system, such as an Ising model.[6] This mapping is particularly attractive because the system can naturally evolve toward low-energy configurations, effectively performing an optimization process, as exemplified by Hopfield neural networks[7] and Boltzmann machines.[8] However, the practical applicability of such methods is fundamentally limited by energetic and entropic barriers:[9,10] as the problem size increases, the number of local minima and saddle points grows exponentially, hindering the system from efficiently reaching the global optimum. Even strategies such as quantum annealing[9,11,12] or simulated annealing (SA)[13] often struggle to overcome these barriers, particularly in large-scale problems.

An alternative strategy for addressing COPs is based on dynamical solvers. In this approach, the binary spin variables $\sigma_i = \pm 1$ are relaxed into continuous analog variables $x_i \in \mathbb{R}$, increasing the system's degrees of freedom and enhancing its ability to escape local minima. Unlike annealing-based methods, which require slow evolution to maximize the probability of reaching the minimum-energy state of the Ising model, dynamical solvers allow the system to evolve on timescales much faster than thermal equilibration or adiabatic processes. In these approaches, the system is driven deterministically toward the lowest-energy state of the corresponding Ising model. This strategy has been demonstrated to be successful in medium- to large-scale optimizations involving up to hundreds of thousands of variables,[14,15] and has even inspired the development of specialized hardware implementations.[16–19]

Building on these developments, experimental and com-

†Corresponding author. E-mail: yuanz@fudan.edu.cn

© 2026 Chinese Physical Society and IOP Publishing Ltd. All rights, including for text and data mining, AI training, and similar technologies, are reserved.

putational implementations of dynamical solvers hold the potential to solve large-scale COPs. Inagaki *et al.*[20] demonstrated a coherent Ising machine (CIM) capable of solving MAX-CUT problems on a 2000-node network, known as K_{2000}, highlighting the advantages of physical dynamical solvers. Goto first proposed a quantum computing scheme based on networks of nonlinear oscillators, in which quantum adiabatic evolution through bifurcation points enables efficient identification of optimal solutions.[21] This approach leverages quantum superposition and fluctuations and draws an analogy to neural networks composed of nonlinear units. Building on this idea, Goto and colleagues subsequently developed a classical algorithm called simulated bifurcation (SB), which emulates adiabatic bifurcations in nonlinear Hamiltonian systems.[22] Implemented on digital hardware such as FPGAs, SB can efficiently solve large-scale COPs, including K_{2000}, with performance surpassing that of previous CIMs. However, continuous dynamical approaches inherently differ from discrete Ising problems: the latter require spins to adopt strictly binary values (± 1), whereas continuous dynamics evolve along smooth trajectories. This mismatch can lead to so-called mapping errors, in which stable continuous trajectories correspond to suboptimal configurations when projected onto the discrete energy landscape.[23] Empirical studies have shown that the interplay between nonlinear dynamical features and the network structure plays a critical role in determining whether the correct solution of the Ising problem can be obtained.[24] To mitigate amplitude heterogeneity, a fully inelastic wall is imposed on the continuous variables x_i in SB, restricting them to the interval $[-1, 1]$. Experimental results demonstrate that two improved versions of SB incorporating the inelastic wall outperform the original algorithm in solving MAX-CUT problems.[14] However, the introduction of the inelastic wall also absorbs system energy, causing the kinetic energy to decay rapidly and limiting the system's ability to escape local minima. To overcome this problem, the Nosé–Hoover method is employed by introducing a thermal bath[25] that replenishes the dissipated kinetic energy. Another approach, the trapping-and-correction method, takes advantage of early-bifurcated "trapped nodes" that maintain their sign throughout the Ising dynamics, effectively reducing computation time.[24] Nevertheless, these methods provide only limited improvement in overcoming the trapping problem.

In this work, we develop a non-Markovian algorithm incorporated into dynamical solvers that significantly enhances the efficiency of searching for optimal or near-optimal solutions. Inspired by studies of system–environment information flow, where non-Markovian backflow from the environment to the quantum system can preserve or restore resources,[26–28] we design a history-dependent negative feedback mechanism, which is also widely employed in neuromorphic computing.[29–32] In our algorithm, the energy dissipated into the environment is partially fed back into the system in the form of a negative feedback force, preventing the system from being trapped in local minima due to rapid loss of kinetic energy. This feedback channel improves the solver's ability to escape local minima and accelerates convergence toward high-quality solutions. We integrate this memory-based force into the ballistic SB (bSB) framework and evaluate its performance on the well-known K_{2000} benchmark, which corresponds to the Sherrington–Kirkpatrick (SK) spin glass model with 2000 fully connected spins.[33] The SK model has been widely adopted to benchmark the performance of Ising solvers due to its high complexity and dense connectivity.[15,20,25,34] Our numerical experiments show that the proposed non-Markovian dynamics effectively alleviates the rapid "freezing" effect induced by the inelastic wall, significantly improving both solution quality and convergence stability, with gains exceeding 60% compared to all existing SB variants. Furthermore, tests on randomly generated SK models with spin numbers ranging from 100 to 1000 confirm that the introduction of non-Markovian dynamics consistently accelerates computational efficiency. Finally, the proposed scheme is also suited for massively parallel hardware implementations, such as field-programmable gate arrays (FPGAs), offering a practical and scalable route to solving large-scale COPs. Here, our focus is primarily on the efficiency and effectiveness of the algorithm itself, rather than its hardware implementation. Investigating detailed hardware realization and associated resource requirements is beyond the scope of this work.

2. Simulated bifurcation for solving MAX-CUT

The MAX-CUT problem is a classical NP-hard COP that has been extensively investigated in theoretical computer science and statistical physics. An undirected weighted graph $G = (V, E)$ is illustrated in Fig. 1(a), where V denotes the set of vertices and E the set of edges connecting them. The task of the problem is to partition the vertices into two disconnected subsets such that the total weight of the edges crossing between the two subsets is maximized. This problem can be equivalently formulated as an Ising spin model, where each vertex is represented by a binary variable $\sigma_i = \pm 1$. The value of the spin then encodes the group to which a vertex is assigned and lowers the overall energy for connected spins i and j if they are in different groups (that is, if $\sigma_i \sigma_j = -1$). In this mapping, maximizing the cut value corresponds to finding the ground state of the Ising Hamiltonian

$$E = -\sum_{i<j} J_{ij} \sigma_i \sigma_j, \tag{1}$$

with $-J_{ij}$ denoting the edge weight. Owing to its dense connectivity and frustrated interactions, particularly in benchmark

models such as the SK spin glass, MAX-CUT provides a stringent testbed for evaluating optimization algorithms and their capability to escape metastable states in rugged energy landscapes.

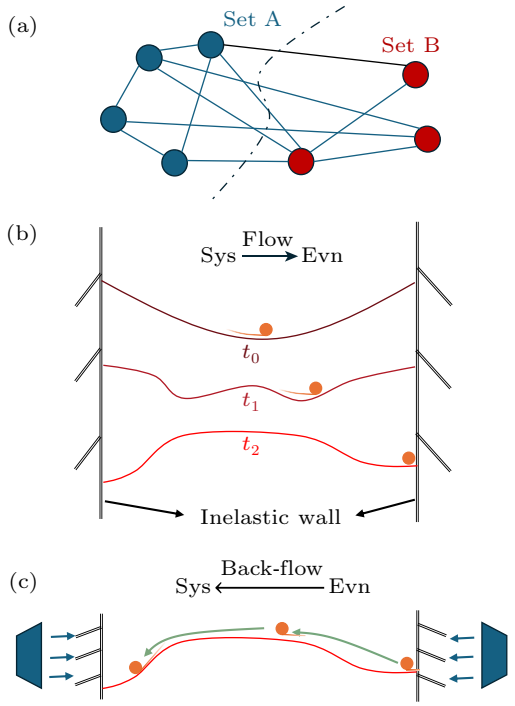


Fig. 1. (a) Schematic of the MAX-CUT problem on an undirected weighted graph, where the objective is to partition the vertices into two disconnected subsets and maximize the sum of edge weights across the cut. (b) Illustration of the inelastic wall constraint in the bSB algorithm: continuous spin variables x_i are restricted to $[-1,1]$, and collisions with the boundary dissipate kinetic energy, potentially trapping the system in local minima. The shadows indicate the system's momentum, which vanishes after collision with the inelastic wall. (c) Illustration of the non-Markovian feedback mechanism: a portion of the dissipated kinetic energy is reinjected into the system through history-dependent negative feedback, providing directed momentum to overcome energy barriers. The arrows on both sides indicate repulsive forces.

SB is a quantum-inspired algorithm that simulates the adiabatic evolution of classical nonlinear Hamiltonian systems.[21,22] It serves as a classical analogue of bifurcation-based adiabatic quantum computation and is widely regarded as one of the most powerful and effective heuristic frameworks for COPs. Its variant, the bSB, further improves performance, achieving both higher solution accuracy and efficiency for the MAX-CUT problem,[14] and is therefore commonly adopted as a representative baseline of state-of-the-art algorithms.

In the bSB, the discrete spin variables of the Ising model are converted into continuous coordinates x_i, with associated momenta y_i, and the system evolves under a Hamiltonian consisting of kinetic and potential energies

$$H = \frac{1}{2}\sum_i y_i^2 + \frac{1-a(t)}{2}\sum x_i^2 - c_0 \sum_{ij} J_{ij} x_i x_j. \tag{2}$$

Here, $a(t)$ is a time-dependent control parameter that gradually increases from zero to 1, guiding the system from a single minimum at the origin toward the energy landscape defined by the Ising term. The continuous spin variables evolve according to Hamiltonian dynamics

$$\dot{x}_i = \frac{\partial H}{\partial y_i}, \quad \dot{y}_i = -\frac{\partial H}{\partial x_i}. \tag{3}$$

Through this adiabatic evolution, the system is ideally expected to progressively approach the ground state of the corresponding Ising Hamiltonian. The coupled differential equations are numerically integrated using the symplectic Euler method[35] with a time step Δt that allows for stable, stepwise updates of the system, enabling the solver to efficiently explore the solution space and effectively escape from local minima.

To address variable heterogeneity — where continuous trajectories may correspond to suboptimal configurations when projected onto the discrete Ising energy landscape — inelastic walls are imposed on the continuous spin variables x_i at ± 1. Whenever $|x_i|$ exceeds 1, the variable is reset to the boundary $[x_i = \mathrm{sgn}(x_i)]$ and its momentum is set to zero $(y_i = 0)$. This constraint stabilizes the system's evolution by preventing excessively large amplitudes that could lead to mapping errors, while still allowing the solver to efficiently explore low-energy configurations and approach the Ising ground state.

However, this mechanism also introduces a severe limitation. As shown in Fig. 1(b), as the control parameter $a(t)$ increases, the potential minimum gradually shifts away from the origin. In certain directions, if a coordinate variable x_i collides with the inelastic wall, its momentum is completely absorbed and the corresponding kinetic energy is immediately transferred from the system into the environment. When a substantial number of variables collide with the walls, the total kinetic energy of the system exhibits a sudden drop. This rapid energy loss leads to insufficient kinetic energy for the system to escape from its current basin of attraction. Consequently, the system is likely to become trapped in a local minimum of the potential energy. Under such conditions, the dynamics effectively "freeze", and the system can no longer evolve toward lower-energy configurations.

To demonstrate this behavior, we conduct numerical experiments on the K_{2000} benchmark — a representative MAX-CUT instance consisting of 2000 fully connected vertices, with each edge assigned a weight of either $+1$ or -1 with equal probability. Figure 2(a) shows the evolution of the cut value during a single trial, with a total evolution length of $N_{\mathrm{step}} = 3000$, where the blue curve represents the standard bSB algorithm. In the initial stage, the bSB rapidly increases the cut value due to its ballistic dynamics, efficiently exploring the solution space and escaping from shallow local minima.

As the system evolves, however, the rate of improvement gradually decreases. Figure 2(b) zooms into the final 1000 steps, showing that the cut value essentially stagnates within

the last 400 steps. This stagnation indicates that the system has already been trapped in a suboptimal local minimum. To further quantify this effect, we plot in Fig. 2(c) the fraction of spin variables that remain active, i.e., those that continue to flip at each time step. The blue curve demonstrates a rapid decline in spin activity: after roughly 2600 steps, nearly all spins have frozen, and the potential energy remains almost unchanged, effectively preventing further increases in the cut value.

This trapping phenomenon is primarily caused by the inelastic wall constraint. As many coordinate variables collide with the walls, their momenta are completely absorbed, resulting in rapid dissipation of kinetic energy into the environment. This quick loss of energy prevents the system from escaping its current basin of attraction, effectively "freezing" the dynamics and halting further progress toward lower-energy configurations. These results clearly illustrate a fundamental limitation of bSB in highly frustrated, large-scale instances: while ballistic dynamics enable fast early-stage convergence, persistent energy dissipation due to hard boundaries restricts the system's ability to continue exploring the solution landscape.

To overcome this limitation, a natural strategy is to partially return the lost energy to the system, allowing it to retain sufficient kinetic energy to escape from local minima. We propose a non-Markovian approach that implements a history-dependent negative feedback mechanism. In this framework, a portion of the energy dissipated into the environment is returned to the system as a directed kinetic boost, compensating for rapid energy loss and preventing the dynamics from freezing in suboptimal basins. Unlike conventional thermal noise, which relies on random fluctuations, this feedback is deterministic and guided by the system's past trajectory, reducing the likelihood of revisiting previously trapped states and enabling more efficient exploration of the energy landscape. By harnessing this memory-based energy recycling, the solver maintains sufficient momentum to overcome energy barriers and approach the global optimum more effectively.

3. The non-Markovian algorithm

To enhance the system's activity for escaping local minima and more effectively exploring the energy landscape, we introduce a directed energy backflow mechanism. In this scheme, a portion of the kinetic energy dissipated to the environment is returned to the system, providing a controlled momentum boost that prevents premature freezing. Specifically, we define a history-dependent energy term for each spin variable

$$K_i = -c_1 x_i \int_{-\infty}^{t} \Gamma\left(t-t'\right) \operatorname{sgn}\left(x_i\left(t'\right)\right) \mathrm{d}t'. \tag{4}$$

Here, c_1 is a positive constant, and Γ is a memory kernel that quantifies how past states influence the current dynamics. In this work, Γ is modelled by an exponentially decaying function, $\Gamma(t-t') = \mathrm{e}^{-\frac{t-t'}{\tau}}$, with the memory time τ. The parameters $\tau = 5$ and $c_1 = 0.04$ are used throughout this work. This design based on Eq. (4) is inspired by spike frequency adaptation in biological neural networks,[36] where the kernel ensures that more recent states exert a stronger influence. The sign function is introduced to maintain sufficient energy even when x_i oscillates in the vicinity of zero, facilitating rapid bifurcation and ensuring adequate energy injection for switching directions during a bifurcation. The memory time τ controls the decay of historical influence: smaller τ emphasizes recent states, whereas larger τ accumulates longer-term history, thereby affecting the efficiency of exploring the energy landscape.

This design ensures that recent states exert a stronger influence on the system's evolution, effectively recycling dissipated energy. As illustrated in Fig. 1(c), by incorporating this non-Markovian feedback, the system receives a history-informed, directed energy backflow, enabling it to overcome energy barriers and reducing the likelihood of repeated trapping in previously visited local minima. Importantly, once the system escapes from a local minimum under the influence of this feedback, the effect does not vanish immediately. Its decay, governed by the memory kernel, provides a delayed influence that prevents the system from returning to the recently escaped minimum. This residual effect further enhances the solver's ability to efficiently explore the energy landscape. Unlike conventional thermal fluctuations, which allow the system to revisit prior configurations without bias, this memory-based dynamics promotes sustained exploration of new regions, thereby increasing the probability of reaching lower-energy states.

We then apply our developed algorithm, which incorporates the non-Markovian feedback mechanism described in Eq. (4), to solve the K_{2000} benchmark. In Fig. 2(a), the red curve shows the cut value of our non-Markovian algorithm during a single trial. Even in the final 1000 time steps (zoomed in Fig. 2(b)), the cut value continues to rise, in contrast to the stagnation observed in the standard bSB. This behavior demonstrates the system's persistent ability to explore higher-quality configurations.

The improved performance of our non-Markovian algorithm is attributed to the history-dependent negative feedback energy term defined in Eq. (4), which corresponds to the returned energy injection. This energy return guarantees the presence of a number of active spins that continue to flip even in the final stages of evolution, as shown by the red curve in Fig. 2(c). This non-Markovian mechanism not only facilitates the system's escape from local minima but also introduces directional persistence, suppressing immediate returns to recently visited minima and thereby significantly enhancing the

capability to explore the energy landscape.

Figure 2(d) presents the distribution of the maximum cut values obtained from 10000 independent trials, each consisting of 3000 evolution steps. The known optimal cut value of 33337 is indicated by a black dash-dotted line. For the standard bSB (blue bars), the distribution is heavily concentrated around a few specific values, with an average of 33203.3 (blue dashed line), reflecting a strong tendency to be trapped in certain local minima. Notably, bSB fails to reach the global optimum in any of the trials, highlighting its limitations in escaping suboptimal basins.

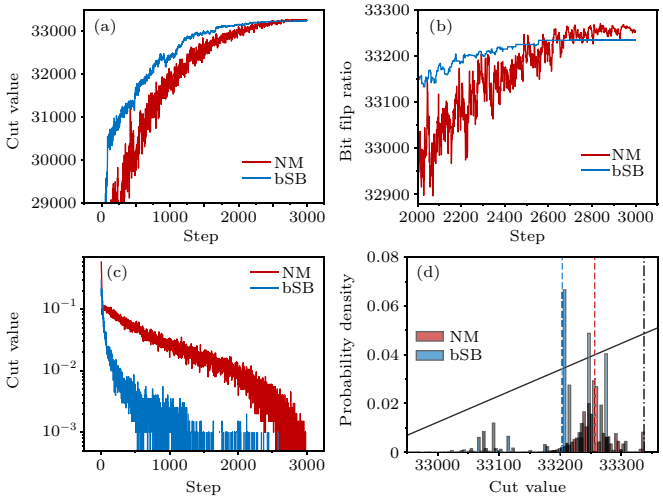


Fig. 2. (a) Evolution of the cut value in a single trial for the K_{2000} benchmark. The blue curve corresponds to the standard bSB algorithm, while the red curve corresponds to the non-Markovian algorithm. (b) Zoom-in of the final 1000 steps, showing that the non-Markovian algorithm continues to increase the cut value, whereas bSB stagnates. (c) Fraction of active spins at each evolution step, illustrating that the non-Markovian algorithm maintains higher spin activity in the later stages compared to bSB. (d) Distribution of cut values obtained from 10000 independent trials. Blue bars correspond to bSB, and red bars correspond to the non-Markovian algorithm. The black dash-dotted line marks the known optimal cut value (33337), and the dashed blue and red lines indicate the average cut values for each method.

In contrast, our non-Markovian algorithm (red bars) produces a broader and more favorable distribution, with an increased average value of 33256.4 (red dashed line), clearly surpassing bSB. Importantly, our method achieves the optimal cut value with a probability exceeding 1%, demonstrating its enhanced ability to explore the energy landscape. This improvement underscores the critical role of the history-dependent feedback mechanism: by returning energy in a trajectory-informed manner, the solver avoids being trapped in prior suboptimal configurations, maintains sustained exploration, and enhances the probability of finding high-quality solutions. Overall, these results provide strong evidence that integrating memory-based feedback significantly boosts both solution quality and reliability in large-scale, frustrated MAX-CUT instances.

To further benchmark our algorithm, we compare it with the standard bSB and the heated bSB (HbSB) algorithm. Figure 3(a) illustrates the performance across varying evolution times, with the known optimal cut value of 33337 marked by a black dashed line. Each step here corresponds to a full evolution from $a(t) = 0$ to a_0. The bSB exhibits rapid convergence in the early stage due to its ballistic dynamics: as $a(t)$ changes quickly (corresponding to smaller N_{step}), the cut value initially increases with evolution time (the blue line and symbols). However, beyond a certain threshold, large-step evolution causes a decline in the cut value. This behavior occurs because, during slow evolution, the majority of spins collide with the inelastic wall at relatively small $a(t)$, leading to rapid kinetic energy dissipation. Consequently, the system becomes trapped even earlier, limiting further exploration of the energy landscape. Despite its fast initial convergence to high-quality suboptimal solutions, bSB is unable to consistently reach the global optimum.

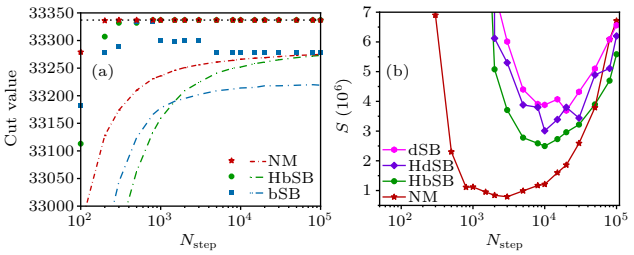


Fig. 3. (a) Comparison of cut values as a function of evolution time for bSB, HbSB, and the non-Markovian algorithm. The lines show the average cut values over 10000 trials, while the symbols represent the maximum cut values. The black dashed line indicates the optimal cut value (33337). (b) Step-to-solution metric S as a function of the number of time steps per trial, quantifying the expected number of sampling steps required to achieve at least one optimal solution with 99% probability. The non-Markovian algorithm demonstrates significantly improved efficiency compared to all SB variants, including HbSB.

The HbSB introduces an additional driving force along the momentum direction, effectively "heating" the system and increasing the kinetic energy. This allows the system to partially overcome local potential barriers, improving the final result. Although HbSB performs better than bSB, it still adopts a Markovian process. The increase in kinetic energy due to heating cannot be efficiently directed. Consequently, HbSB can temporarily escape from some local minima, but it is challenging for the system to rapidly reach the global energy minimum. In addition, HbSB converges more slowly than bSB with respect to the number of steps. Our non-Markovian algorithm consistently outperforms both bSB and HbSB. It achieves the optimal cut value in just 300 evolution steps, whereas HbSB requires at least 800 steps under the same conditions. Moreover, the average cut value of our method is always higher across all evolution speeds, demonstrating that the history-dependent feedback prevents premature freezing and promotes sustained directional exploration.

The performance of the solver can be quantified using the so-called step-to-solution (S) metric

$$S = N_{\text{s}} \cdot \frac{\log 0.01}{\log (1 - P)}. \tag{5}$$

It denotes the expected number of sampling steps required to achieve at least one optimal solution with 99% probability. In Eq. (5), P is the empirical success probability, and N_s is the number of steps per trial. Unlike the commonly used time-to-solution metric, step-to-solution reflects the intrinsic sampling efficiency of the algorithm itself, independent of hardware update speed.

Figure 3(b) shows S versus the number of steps for our non-Markovian algorithm compared with SB variants, including HbSB, the diffusive SB (dSB), and the heated dSB (HdSB). Here, we do not consider the standard bSB, because it fails to reach the optimum under all evolution speeds. Our non-Markovian method significantly outperforms all SB variants. Among them, HbSB exhibits the best performance with $S = 2.5 \times 10^6$ at $N_{\text{step}} = 10000$. In contrast, our non-Markovian approach achieves $S = 7.9 \times 10^5$ at $N_{\text{step}} = 3000$, representing a 64.8% improvement. These results clearly demonstrate the advantage of incorporating non-Markovian energy backflow: by effectively leveraging information from past trajectories, the system can traverse energy barriers more efficiently, reduce the likelihood of being repeatedly trapped in local minima, and accelerate convergence toward the global optimum.

4. Performance across SK models with different sizes

All the above investigations focused on the SK Ising problem K_{2000}, and we next evaluate the performance of our proposed non-Markovian method for system sizes ranging from 100 to 1000 spins, all connected in an all-to-all fashion. The choice of fully connected graphs is intended to make the problem as challenging as possible, thereby rigorously testing the capability and robustness of the algorithm. For each system size, 100 randomly generated instances are used to ensure statistical significance. To obtain reliable estimates of the step-to-solution metric, reference solutions are first computed using simulated annealing (SA) with sufficiently long annealing times and a large number of iterations, ensuring that the solutions closely approximate the global optimum. Each instance is then independently solved across 1000 trials, with the highest cut value recorded for each run. All algorithmic parameters are kept consistent with those optimized for K_{2000} to allow a fair comparison. [25] The results are summarized in Fig. 4, presenting both the probability of achieving the optimal solution (Fig. 4(a)) and the average step-to-solution S (Fig. 4(b)) as a function of system size, with a total evolution length of $N_{\text{step}} = 800$. Across all problem sizes, our non-Markovian algorithm consistently outperforms the previously best-performing HbSB variant. Notably, the relative performance advantage grows with increasing system size, highlighting that the benefits of history-dependent feedback scale favorably with problem complexity.

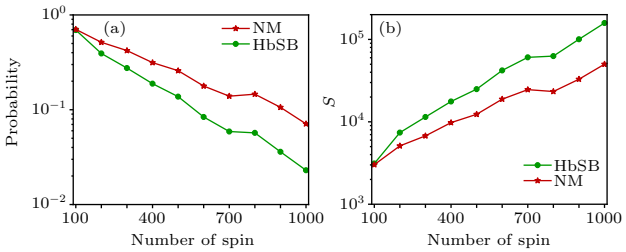


Fig. 4. Performance of the non-Markovian algorithm on SK Ising problem instances with system sizes ranging from 100 spins to 1000 spins. For each system size, 100 random instances were generated and solved independently across 1000 trials. (a) Probability of achieving the optimal solution. (b) Average step-to-solution metric S as a function of system size. The results indicate that the non-Markovian algorithm consistently outperforms the best-performing HbSB variant, with performance benefits increasing for larger system sizes, demonstrating scalable improvements in solution quality and computational efficiency.

These results demonstrate that the non-Markovian mechanism provides both improved solution quality and computational efficiency. Importantly, the method scales robustly with system size, making it a highly promising approach for solving large-scale, densely connected combinatorial optimization problems where conventional solvers or standard SB variants may struggle. Overall, the integration of history-informed energy backflow not only accelerates convergence but also ensures more reliable attainment of global optima, underscoring the practical utility of this approach for complex optimization tasks.

All numerical simulations in this work were performed on a MacBook Air equipped with an Apple M3 CPU running at 3.2 GHz. Other solvers adopt previously optimized settings reported in Ref. [25], with $\Delta t = 0.7$ and $c_0 = 0.6$ for bSB, $\Delta t = 1.1$ and $c_0 = 0.6$ for dSB, and $\Delta t = 1.1$ and $c_0 = 0.9$ for HbSB. For the proposed method, we adopt $\Delta t = 1.3$ and $c_0 = 0.6$. These details ensure that all reported results are fully reproducible.

5. Conclusion

In this work, we have introduced a non-Markovian memory-based feedback mechanism for dynamical solvers tackling COPs, exemplified by MAX-CUT instances on fully connected SK spin glass models. By returning a portion of the dissipated kinetic energy into the system in a history-dependent, trajectory-informed manner, our method effectively suppresses the early freezing problem caused by the inelastic wall constraints in the standard bSB.

Numerical experiments on the K_{2000} benchmark demonstrate that the non-Markovian algorithm maintains higher spin activity throughout the evolution, consistently increases the cut values beyond those achievable by bSB and HbSB, and achieves the global optimum with a non-negligible probability.

Compared to existing SB variants, our approach significantly reduces the step-to-solution metric, yielding up to 64.8% improvement in computational efficiency. Furthermore, tests on randomly generated SK instances of varying sizes (from 100 to 1000 spins) confirm that the benefits of memory-based feedback scale favorably with system size, enhancing both the probability of finding the optimal solution and the efficiency of exploration.

The integration of non-Markovian dynamics offers a robust and scalable strategy for solving large-scale, densely connected COPs. By leveraging past trajectory information to guide energy backflow, our method not only accelerates convergence but also ensures more reliable attainment of global optima, highlighting its potential for practical implementation on specialized hardware platforms such as FPGAs. This work establishes a general framework for history-informed dynamical solvers and opens avenues for further exploration of non-Markovian effects in optimization and beyond.

Acknowledgments

This project was supported by the National Key Research and Development Program of China (Grant No. 2024YFA1408500), the National Natural Science Foundation of China (Grant Nos. 12174028 and 12574115), and the Open Fund of the State Key Laboratory of Spintronics Devices and Technologies (Grant No. SPL-2408).

References

[1] Mezard M, Parisi G and Virasoro M A 1987 *Spin Glass Theory and Beyond* (Singapore : Singapore World Scientific)
[2] Barahona F, Gröschel M, Jünger M and Reinelt G 1988 *Oper. Res.* **36** 493
[3] Chang K C and Du D H C 1987 *IEEE Trans. Comput. Aided Des. Integr. Circuits Syst.* **6** 67
[4] Wang J, Jebara T and Chang S F 2013 *J. Mach. Learn. Res.* **14** 771
[5] Collins T 2004 *Graph Cut Matching in Computer Vision* (Edinburgh: University of Edinburgh)
[6] Lucas A 2014 *Front. Phys.* **2** 5
[7] Hopfield J J 1982 *Proc. Natl. Acad. Sci. USA* **79** 2554
[8] Aarts E H L and Korst J 1989 *Simulated Annealing and Boltzmann Machines* (Chichester: Wiley)
[9] Bellitti M, Ricci-Tersenghi F and Scardicchio A 2021 *Phys. Rev. Res.* **3** 043015
[10] Monasson R, Zecchina R, Kirkpatrick S, Selman B and Troyansky L 1999 *Nature* **400** 133
[11] Albash T and Lidar D 2018 *Rev. Mod. Phys.* **90** 015002
[12] Santoro G E, Martonak R, Tosatti E and Car R 2002 *Science* **295** 2427
[13] Kirkpatrick S, Gelatt C D and Vecchi M P 1983 *Science* **220** 671
[14] Goto H, Endo K, Suzuki M, Sakai Y, Kanao T, Hamakawa Y, Hidaka R, Yamasaki M and Tatsumura K 2021 *Sci. Adv.* **7** eabe7953
[15] Honjo T, Sonobe T, Inaba K, Inagaki T, Ikuta T, Yamada Y, Kazama T, Enbutsu K, Umeki T, Kasahara R, Kawarabayashi K and Takesue H 2021 *Sci. Adv.* **7** eabh0952
[16] Okawachi Y, Yu M, Jang J K, Ji X, Zhao Y, Kim B Y, Lipson M and Gaeta A L 2020 *Nat. Commun.* **11** 4119
[17] Tatsumura K, Dixon A R and Goto H 2019 *29th International Conference on Field Programmable Logic and Applications (FPL)* 59
[18] Yamaoka M, Yoshimura C, Hayashi M, Okuyama T, Aoki H and Mizuno H 2016 *IEEE J. Solid-State Circuits* **51** 303
[19] Mohseni N, McMahon P L and Byrnes T 2022 *Nat. Rev. Phys.* **4** 363
[20] Inagaki T, Haribara Y, Igarashi K, Sonobe T, Tamate S, Honjo T, Marandi A, McMahon P L, Umeki T, Enbutsu K, Tadanaga O, Takenouchi H, Aihara K, Kawarabayashi K-I, Inoue K, Utsunomiya S and Takesue H 2016 *Science* **354** 603
[21] Goto H 2016 *Sci. Rep.* **6** 21686
[22] Goto H, Tatsumura K and Dixon A R 2019 *Sci. Adv.* **5** eaav2372
[23] Leleu T, Yamamoto Y, McMahon P L and Aihara K 2019 *Phys. Rev. Lett.* **122** 040607
[24] Wang J, Ebler D, Wong K Y M, Hui D S W and Sun J 2023 *Nat. Commun.* **14** 2510
[25] Kanao T and Goto H 2022 *Commun. Phys.* **5** 212
[26] De Vega I and Alonso D 2017 *Rev. Mod. Phys.* **89** 015001
[27] Breuer H P, Laine E M, Piilo J and Vacchini B 2016 *Rev. Mod. Phys.* **88** 021002
[28] Mendonca T M, Celeri L C, Paternostro M and Soares-Pinto D O 2024 *Phys. Rev. A* **110** L040401
[29] Miao Y, Zhao L, Zhang Y and Yuan Z 2025 *Sci. China Phys. Mech. Astron.* **68** 217511
[30] Zhao L, Zhang M, Zhang Y, Mi Y, Yuan Z and Xia K 2024 *Phys. Rev. Appl.* **21** 064040
[31] Zhang Y, Zheng Q, Zhu X, Yuan Z and Xia K 2020 *Sci. China Phys. Mech. Astron.* **63** 277531
[32] Qiao Y, Zhang Y and Yuan Z 2023 *New J. Phys.* **25** 033031
[33] Sherrington D and Kirkpatrick S 1975 *Phys. Rev. Lett.* **35** 1792
[34] Aramon M, Rosenberg G, Valiante E, Miyazawa T, Tamura H and Katzgraber H G 2019 *Front. Phys.* **7** 48
[35] Leimkuhler B and Reich S 2004 *Simulating Hamiltonian Dynamics* (Cambridge : Cambridge University Press)
[36] Benda J and Herz A V M 2003 *Neural Comput.* **15** 2523